

Glitching pulsars: unraveling the interactions of general relativity with quantum fields in the strong field regimes

A. A. Hujeirat*

IWR, Universität Heidelberg, 69120 Heidelberg, Germany

R. Samtaney†

Applied Mathematics and Computational Science,

King Abdullah University of Science and Technology, Thuwal 23955-6900, Saudi Arabia

(Dated: February 2, 2022)

Abstract

We present a modification of our previous model for the mechanisms underlying the glitch phenomena in pulsars and young neutron stars. Accordingly, pulsars are born with embryonic cores comprising of purely incompressible superconducting gluon-quark superfluid (henceforth SuSu-cores). As the ambient medium cools and spins down due to emission of magnetic dipole radiation, the mass and size of SuSu-cores are set to grow discretely with time, in accordance with the Onsager-Feynmann analysis of superfluidity. Presently, we propose that the spacetime embedding glitching pulsars is dynamical and of bimetric nature: inside SuSu-cores the spacetime must be flat, whereas the surrounding region, where the matter is compressible and dissipative, the spacetime is Schwarzschild. It is further proposed that the topological change of spacetime is derived by the strong nuclear force, whose operating length scales is found to increase with time to reach $\mathcal{O}(1)$ cm at the end of the luminous lifetimes of pulsars. The model presented here model is in line with the recent radio and GW observations of pulsars and NSs.

*Electronic address: AHujeirat@uni-hd.de

†Electronic address: Ravi.Samtaney@kaust.edu.sa

I. INTERNAL STRUCTURE OF UCSS

Pulsars, neutron stars (NSs) and magnetars build the family of ultra-compact stars (UCSs) with compactness parameter, α_S , generally larger than half. Recalling that the average density of matter in the interiors of UCSs is larger than the nuclear one, ρ_0 , then these objects are well-suited for probing the interaction of general relativity with quantum fields in the strong field regime. In fact,

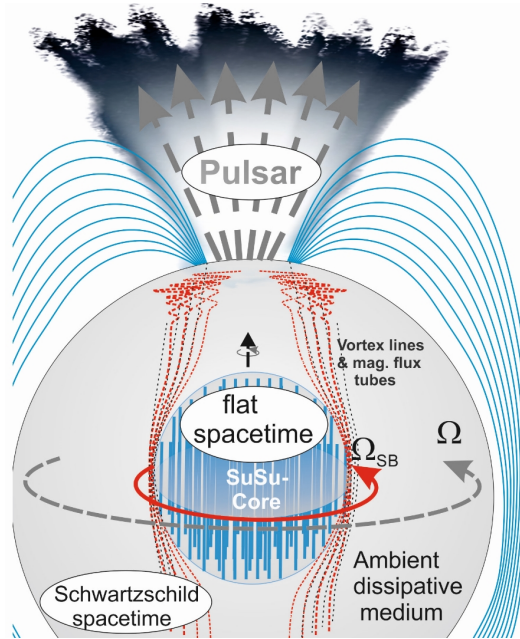


FIG. 1: Schematic depiction of the internal structure of glitching pulsars. Pulsars are born with embryonic cores comprised of an incompressible gluon-quark superfluid and embedded in flat spacetime. The overlying shells are made of dissipative and compressible quantum fluid, but embedded in Schwarzschild spacetime.

pulsars and NSs have been successfully used for probing general relativity, such as the emission of gravitational waves (GWs) in binary pulsars and direct detection GWs through merger of neutrons stars and black holes (see [1] and [19] for detailed reviews). However, the internal structure of UCSs continues to be a mystery and remains a challenge for astrophysicists (see the review in [21] and the references therein). On the other hand, the observed glitch-phenomena associated with pulsars are events that may be considered to be connected to the dynamics of matter inside their interiors (see [3, 6, 12, 21] and the references therein). However, based on observations and theoretical arguments, one may try to constrain the nature of matter inside normal UCSs as follows:

1. The observed spin-down of UCSs results from the loss of magnetic and rotational energies that

are estimated to be of order 10^{38} erg/s. This would imply complete exhaustion of the stored removable energies¹ inside pulsars within about ten million years, provided that the heat conductivity operates on length scales that are larger than the nuclear ones. Consequently, very old and isolated UCSs, including those formed through the collapse of the first generation of stars, must be by now dark and invisible and therefore excellent black hole candidates. This argument would explain why neither UCSs nor black holes in the mass range $[2M_{\odot} \leq \mathcal{M} \leq 5M_{\odot}]$ have ever been observed.

2. The rest of thermal, kinetic and magnetic energies that are left from the collapse of the progenitors of UCSs are transported outwards into the outer shells and subsequently liberated away. In the absence of nuclear energy generation, the Tolman-Oppenheimer-Volkoff equation (TOV-equation) may still accept a positive gradient of the thermal energy, turning the central core to be the coldest region inside the object and thereby facilitating a phase transition of the compressible dissipative nuclear matter into incompressible superfluid. Such a transition may still occur even when the matter's temperature is still beyond several million degrees.
3. Theoretical studies show that in the regime of nuclear density and beyond, almost all EOSs used for modeling state of matter in the interiors of UCSs tend to converge to the limiting case $\varepsilon = P$ (see [6] and the references therein). However, this state corresponds to pure incompressible fluids [14]. Due to causality and stability reasons, except rest energy, the incompressible fluid should be free of all other removable energies, such as thermal, kinetic and magnetic energies. Hence, the core is expected to end up as a condensate with zero-entropy, whose constituents communicate with each other at the speed of light and therefore the momentum exchange between them must saturate around a universal maximum. In this case, the coupling constant in the context of asymptotic freedom in QCD would converge to its universal minimum value, where quarks should be moving freely throughout the whole domain [11, 20]. Such a zero-entropy superfluid² cannot accept spatial variations or stratification due to gravity, and therefore the embedding spacetime must be flat. This state may be maintainable, if the involved quarks are attached to a spatially fixed lattice, where they may behave collectively as a single macroscopic quantum entity. Indeed, although both entropy and energy states of colliding protons at the RHIC and LHC differ significantly from those at

¹ i.e. energies other than rest energy

² vanishing energy loss due to acceleration/deceleration should be excluded

the centers of UCSs, these experiments have shown that the properties of the resulting fluids mimic those of perfect fluids (see [5, 23] for further details).

4. Based on astronomical observations, there appears to be a gap in the mass spectrum of ultra-compact objects: neither black holes nor NSs have ever been observed in the mass range $[2\mathcal{M}_\odot < \mathcal{M} < 5\mathcal{M}_\odot]$. Moreover, intensive astronomical observations of the newly detected NS-merger GW170817 [1] failed to unambiguously classify whether the resulting object is a stellar black hole or a NS. These both facts are in line with our scenario that pulsars and young neutron stars evolve on the cosmological time scale into massive dark energy objects that become indistinguishable from stellar black holes. A schematic description of the scenario is shown in Figs. (1, 2) and (4).

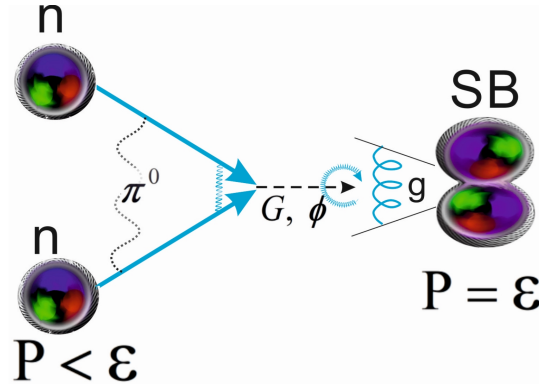


FIG. 2: Neutron merger at the centers of pulsars. The compressible and dissipative neutron fluid is governed by equations of state (EOSs) in which the pressure $P < \varepsilon$. When the density approaches the critical density, ρ_c , then the EOS changes into $P = \varepsilon$, which corresponds to incompressible quantum fluid. At $\rho = \rho_c$, it is energetically favourable for neutrons to begin deconfining the quarks and merge together to form an ocean of gluon-quark superfluid, though the resulting global gluon cloud must be much more energetic.

A. The model and the governing equations

For modeling the internal structure of pulsars, the general relativistic field equations should be solved;

$$G_{\mu\nu} = \kappa T_{\mu\nu}, \quad \text{for } \mu, \nu : 0 \rightarrow 4, \quad (1)$$

where $G_{\mu\nu}$, $T_{\mu\nu}$ are the Einstein and the Stress-Energy tensors, respectively, and κ is a coefficient. The rotational, magnetic, thermal and other energies in UCSs are generally about three orders of magnitude smaller than the rest energy and therefore they may be safely neglected. In this case, Schwarzschild spacetime is most suited for modelling their internal structures. Hence, the corresponding metric reads:

$$ds^2 = e^{2\nu(r)} dt^2 - e^{2\lambda(r)} dr^2 - r^2 d\Omega^2, \quad (2)$$

where $d\Omega = d\theta^2 + \sin^2\theta d\varphi^2$ is a surface element on a sphere of radius “r”. The field equations can then be reduced to just one single equation, i.e. the so-called Tolman-Oppenheimer-Volkoff (TOV) equation:

$$\frac{dP}{dr} = -\frac{G}{c^4 r^2} \frac{[\varepsilon + P][m(r) + 4\pi r^3 P]}{1 - r_s/r}, \quad (3)$$

where r , r_s , G , P , $m(r)$ correspond to the radius, Schwarzschild radius, gravitational constant, pressure and the dynamical mass, respectively (see Sec. (4) in [14] for further details).

Recalling that GR is incapable of modeling gravitationally bound incompressible matter, then the spacetime embedding pulsars may be decomposed into two separate domains: a flat spacetime that embeds the SuSu-core and a surrounding Schwartzschild spacetime that embeds the ambient media as mentioned above. The decomposition of the domain is motivated by relativistic causality which prohibits fluid stratification or spatial variation of the density of purely incompressible fluids; hence the spacetime embedding the core must have zero-curvature, i.e. purely flat.

Based thereupon the line element in the core is described by the metric in spherical polar coordinates (t, r, θ, φ) :

$$ds^2 = c^2 dt^2 - dr^2 - r^2 d\Omega^2. \quad (4)$$

The physical properties of the SuSu-core are set to affect the structure of the ambient medium by allowing $m(r)$ and r_s in the TOV-equation to depend on the total enclosed mass, i.e. on $m(r) = M_{SuSu} + 4\pi \int_{r=r_{SuSu}}^{\infty} \rho r^2 dr$.

On the other hand, as the matter in the rotating core is in incompressible superfluid state, it must contain a discrete array of vortices. Their total number, N , the mass and size growth of the core are determined through the Onsager-Feynmann equation for modeling quantized circulations:

$$\oint v \cdot d\ell = \frac{2\pi\hbar}{m^*} N, \quad (5)$$

where v , ℓ , \hbar , m^* , N correspond to rotational velocity, line-element along the circular path, the reduced Planck constant, the mass of the superfluid particles and the enclosed number of vortices, respectively [9, 22].

Inside the core, the quantum fluid is assumed to have zero-entropy and has reached the critical supranuclear density, $\rho = 3\rho_0$, beyond which merger of individual gluon clouds into a global one becomes possible. The effective energy of the latter cloud correlates linearly with the number of merged neutrons, i.e.

$$\sum_1^N E_n^0 \xrightarrow{\text{mergering process}} \sum_1^N E_n^0 + N \times \Delta E_{bag}, \quad (6)$$

where ΔE_{bag} is the bag energy enhancement needed to confine the quarks inside the super-baryon and N denotes the total number of merged neutrons to forming the super-baryon, E_n is the rest energy of a single neutron. In this case the energy and pressure of the incompressible gluon-quark superfluid inside the core are as follows: $\varepsilon_{tot} = \varepsilon_0 + \varepsilon_\phi$, $P_{tot} = P_0 + P_\phi$, where ε_0 is the energy density of the baryonic matter and $\varepsilon_\phi = \frac{1}{2}\dot{\phi}^2 + V(\phi) + \frac{1}{2}(\nabla\phi)^2$ and $P_\phi = \frac{1}{2}\dot{\phi}^2 - V(\phi) + \frac{1}{6}(\nabla\phi)^2$ are the energy density and pressure of the scalar field, which are assumed to be identical to ΔE_{bag} . As the matter inside the cores of pulsars is set to be incompressible and stationary, it is reasonable to assume $\phi = \text{constant}$. In this case, $\dot{\phi}$ and $\nabla\phi$ must vanish and $V(\phi)$ can be considered as the energy density required for deconfining the quarks inside the super-baryon, i.e., the SuSu-core. Here we set $\varepsilon_{tot} = 2\varepsilon_0$, whereas the pressure $P_{tot} = P_0 - V(\phi) = \varepsilon_0 - V(\phi) = 0$. Thus, the total local pressure of incompressible gluon-quark superfluid inside SuSu-cores vanishes completely. Exterior to the core, the matter is said to be baryonic, dissipative, compressible and embedded in a Schwarzschild spacetime.

1. Initial and boundary conditions

The present scenario is based on a previous model for the origin of glitches in pulsars. Accordingly, pulsars and young neutron stars are expected to undergo billions of glitch events during their luminous lifetimes before ending as ultra-compact and invisible dark energy objects. In the present study, we select several epochs in the lifetimes of pulsars and the corresponding internal structures are calculated subject to the following conditions:

- ◆ The pulsar has the initial mass of $1.33\mathcal{M}_\odot$, made of a purely baryonic compressible matter.
- ◆ The pulsar is set to have initially the compactness parameter $\alpha_s = 1/2$.

- ◆ The central baryonic density is set to be equal to the critical $\rho_c = 3 \rho_0$, at which a transition into quark deconfinement occurs, and where the Gibbs function vanishes.
- ◆ The dissipative and compressible baryonic matter is set to obey the polytropic EOS: $P = \mathcal{K} \rho^\gamma$.

The selected models correspond to pulsar phases in which the enclosed SuSu-cores have reached the following radii: $R_{SuSu} = 0.333, 0.525, 0.78525$ and 0.8575 in units of $[\tilde{R} (= R_S/\alpha_s)]$, where R_S is the corresponding Schwarzschild radius. The total density inside SuSu-cores amounts to: $\rho_{tot} = \rho_b + \rho_\phi = 2 \rho_c \approx 6 \rho_0$.

1. Model-0: The pulsar is made of purely baryonic matter. Here, the TOV-equation is solved for the pressure starting from a given $P(r=0) = P_0$ up to a radius, where the pressure vanishes.
2. Combined-models: The pulsar models are made both of SuSu-cores surrounded by dissipative and compressible quantum fluid. The radii of the cores are: $R_{SuSu} = 0.333, 0.525, 0.78525, 0.8575$. The total mass of the core is calculated through the integration:

$$m_{tot}(r = R_{core}) = \int_0^{R_{core}} (\varepsilon_b + \varepsilon_\phi) dr. \quad (7)$$

The solutions here are based on adapting the parameters \mathcal{K} and γ of the EOS in a manner such that the initial baryonic mass of $1.33 \mathcal{M}_\odot$ the pulsar remains preserved.

3. The ultimate final phase: Here the radius and mass of the SuSu-core are roughly equal to the critical values: $R_{SuSu} = 0.859 \approx R_{Schw.}$ and $M_{SuSu} \approx M_{Schw.}$. Here the initial pulsar must have metamorphosed entirely into an invisible SuSu-object.

2. Results

For enhancing the spatial accuracy of the calculations, an explicit adaptive mesh refinement (EAMR) has been developed, in which the aspect ratio, dr_{max}/dr_{min} , may reach 100 million. Unlike dynamic adaptive mesh refinement (AMR), EAMR is based on *a posteriori* refining the grid distribution in certain locations of the domain, where the gradients of the physical variables are large. This may be achieved by manually manipulating the grid distribution and restarting the calculations anew. In the present case, for example, the location where the pressure vanishes is vitally important and therefore the resolution should be maximally refined (Fig.3). Unlike AMR, solution methods based on EAMR generally converge much faster than their AMR-counterparts,

hence contributing to the global efficiency and robustness of the numerical solution procedure (see [24] and the references therein).

Based on the previous study [18], five episodes in the cosmological evolution of pulsars have been selected (see Fig. 4). For each episode, the TOV equation, modified to include dark energy input at the background of the here-presented bimetric scenario of spacetime, has been solved.

In Figs. (5, 6) the profiled of the corresponding five runs are displayed. In Figs. 5 and 6) show the profile of pressure and total energy density, respectively, for five different runs. These are based on the aforementioned bimetric scenario of spacetime. Profile (1) corresponds to the radial distribution of the pressure obtained by solving the TOV equation. The phase here corresponds to the moment of birth of the pulsar, when it is entirely embedded in a Schwartzschild spacetime. Profiles (2, 3, 4 and 5) in Fig.(5) show the radial distributions of the pressure at different epochs, specifically when the SuSu-core has grown in mass and size to reach the sequence of radii: $R_{SB} = 0.333, 0.525, 0.78525$ and 0.7875 . Note that as the SuSu-core becomes more massive, the curvature of spacetime embedding the ambient medium is enhanced, which, in turn, compresses the ambient medium even more, thereby reducing the effective radius of the pulsar. This would explain the mass-radius relations displayed in Figs. 7 and 8. Here the corresponding Schwarzschild radius increases and propagates outwards to finally meet the decreasing radius of the contacting pulsar. The overlapping of the both radii is expected to occur at the end of the pulsar's luminous lifetime (see Fig. 4 and Profile 5 in Figs.(5)).

As purely incompressible superfluids in flat spacetime have zero-spatial variations (see Fig.(9), then the gravitational potential inside SuSu-cores should attain a sequence of constant values. Their magnitudes correlate with the mass and size of the SuSu-core. As a consequence, as the SuSu-core becomes more massive, the gravitational redshift of the pulsar increases as well to finally reach very large values at the end of the pulsar's luminous lifetime (see Profile "6" in Fig.10). Here the Schwarzschild radius becomes almost equal to the effective radius of the object, enforcing the object to sink deeply in spacetime and becomes invisible.

Note that the profiles shown in Figs.(9 and 10) are not just schematic representations, but rather have been obtained using direct numerical computations.

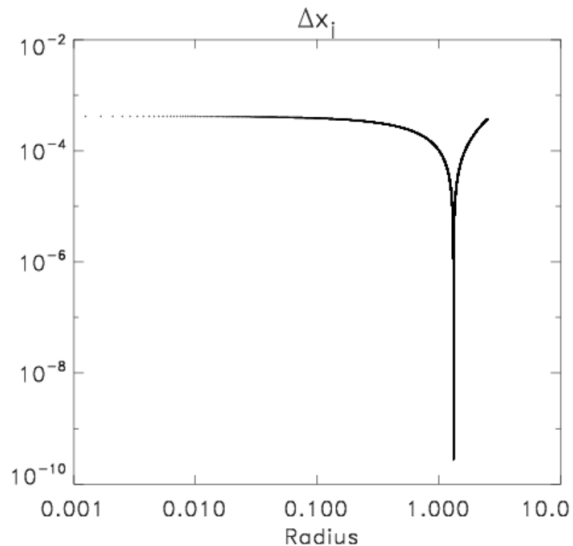


FIG. 3: The distribution of the finite volume cells as function of radius. Here the explicit adaptive mesh refinement (EAMR) has been employed to increase the accuracy at both the interface between the core and the ambient medium as well as to outer radius of the object.

II. SUMMARY AND DISCUSSION

The pulsar model presented here is analogous to a terrestrial experiment of a rotating superfluid Helium in a container. While the SuSu-matter inside the core corresponds to a rotating superfluid Helium, the dissipative ambient medium would be represented by the solid container. However, the pulsar model here is much more sophisticated, as quantum and general relativistic effects are taken into account. In the following we discuss the main features of the model:

- For $\rho \geq \rho_{crit}$, neutrons at the center of pulsars are set to merge together to form an incompressible gluon-quark superfluid, governed by the EOS $P = \varepsilon$. This argument is supported by the following observations:
 - ◇ Theoretical studies of nuclear interactions in the regime $\rho \geq \rho_0$ show that almost all EOSs converge to the limiting case: $P = \varepsilon = a_0 n^2$, which corresponds to the pure incompressible state. However, once the matter is governed by $P = \varepsilon$, the chemical potential μ would achieve a universal maximum, i.e. $\frac{\partial \mu}{\partial n} = 0$.
 - ◇ based on thermodynamical considerations, it was shown in [14] that at $\rho = \rho_{crit} \approx 3 \times \rho_0$, in combination with zero-entropy condition, the Gibbs function attains a global zero-minimum, facilitating thereby a crossover phase transition into a globally confined gluon-

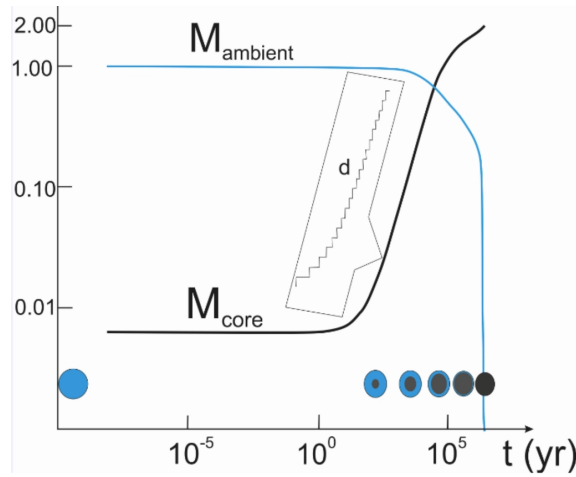


FIG. 4: Based on the solution of the TOV equation in combination with Onsager-Feynmann equation, the size and mass of SuSu-cores grow with time following a well-defined mathematical sequence $\{\alpha_c^n\}$. The discrete increase of \mathcal{M}_{core} is magnified and shown “d”. To verify the bimetric model of pulsars, six epochs with different core-sizes have been selected: a newly born pulsar, four intermediate phases and the final massive state, where the whole object turns into an invisible dark energy object.

quark superfluid, where $\frac{\partial \mu}{\partial n} = 0$.

- The formation of incompressible gluon-quark superfluids is associated with energy enhancement of the gluon field at the surface of the core, which is needed for globally re-confining the enclosed quarks, thereby effectively enhancing the effective mass of the core.
- The phase transition of the quantum fluid in the boundary layer (BL) from compressible-dissipative into incompressible superfluid states is associated with changes of the spacetime topology from a curved spacetime into a purely flat one. The latter reaction is due to causality, which prohibits incompressible superfluids to be embedded by a curved spacetime. Indeed, the topology change of spacetime is associated with the emission of gravitational waves. However, due to the tiny little volume of the BL, the detection of GW-emission during glitch-events would be much below the sensitivity of today GW-detectors.
- Both the phase transition of matter and the change of topology of spacetime are provoked by the SNF, which appear to develop into a macroscopic force as the pulsars age. In fact, as the core is made of SuSu-matter, the core is equivalent to a super-baryon, in which the enclosed quarks are shielded by a gluon cloud [13]. As will be shown later, the SNF transmitted by this

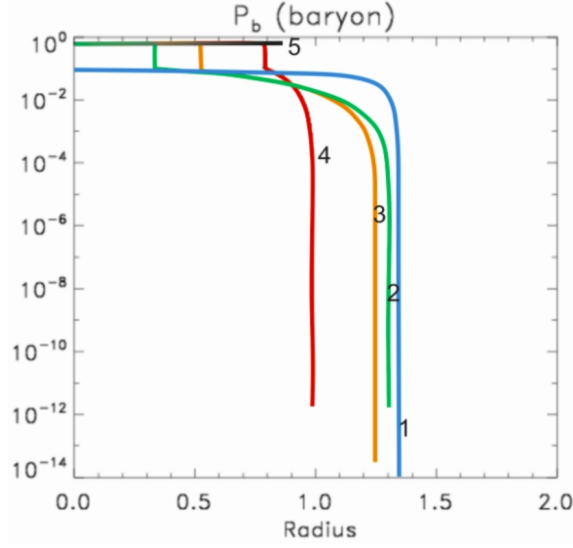


FIG. 5: The distribution of the baryonic pressure inside an evolving pulsar after five selected glitch events at different epochs. Inside the core, in addition to the rest energy of the baryonic matter, there is an energy enhancement due to the scalar field, which is equivalent to the additional energy required for re-confining the sea of quarks. The transition between both regions is not smooth as the matter inside the core evolves quantum mechanically, whereas the ambient medium obeys the normal laws of continuum.

cloud is found to correlate nicely with the size and mass of the core. The neutrons in the BL become increasingly locked to the core, thereby adapting the physical conditions of the matter inside the core. Following the scenario of [18], the occurrence of glitches in pulsars follows a well defined sequence, whose elements are $\{\alpha_c^n\}$ where $\alpha_c^n = \Omega_c^n / \Omega_c^{n+1} = 1 + (\Delta\Omega / \Omega)^n$, and $n : 0 \rightarrow \infty$. Here $n = 0$ corresponds to the first glitch event immediately after the pulsar's formation, whereas $n = \infty$ corresponds to the final glitch event at the end of the pulsar's luminous lifetime.

Thereupon, let R_n, Ω_n be the radius and angular frequency of the SuSu-core on the verge of the glitch event number " n ", respectively. The rotational energies of the SuSu-core at time t_n and t_{n+1} read:

$$\begin{aligned} E_{rot,SB}^n &= \frac{4\pi\rho_{crit}}{15} R_n^5 \Omega_n^2 \\ E_{rot,SB}^{n+1} &= \frac{4\pi\rho_{crit}}{15} R_{n+1}^5 \Omega_{n+1}^2. \end{aligned}$$

From conservation of rotational energy: $E_{rot,SB}^n = E_{rot,SB}^{n+1}$, we obtain the relation:

$$\left(\frac{R_{n+1}}{R_n}\right)^5 = \left(\frac{\Omega_n}{\Omega_{n+1}}\right)^2. \quad (8)$$

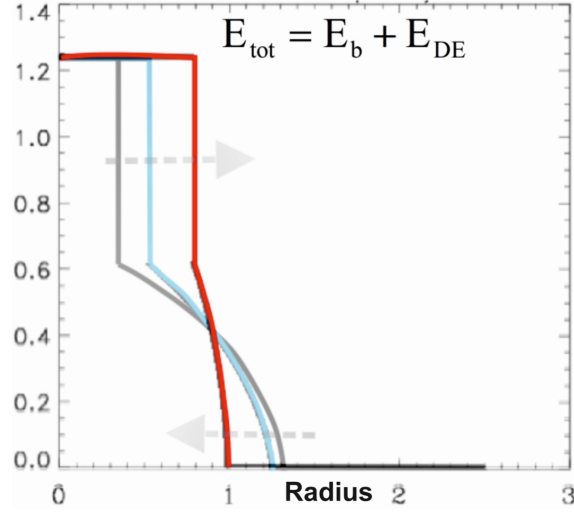


FIG. 6: Similar to the previous figure: the distribution of the total energy density inside both the core and the ambient dissipative medium are shown.

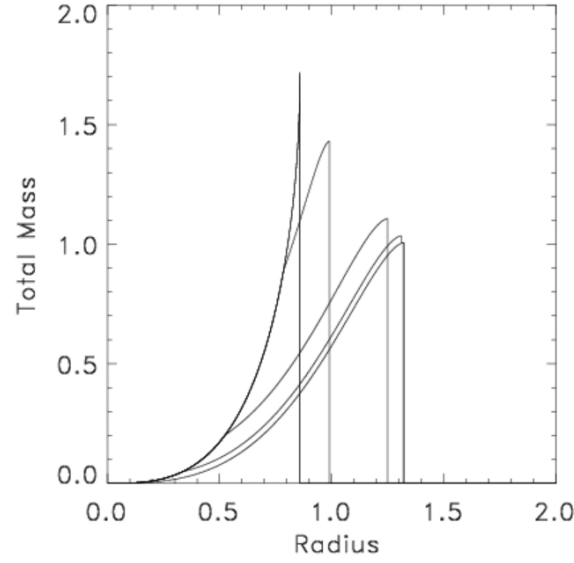


FIG. 7: The total enclosed mass of the object versus radius after selected glitch events. As the mass of the SuSu-core increases, its compactness of the whole object increases as well to finally reach the critical Schwarzschild mass.

Inserting $R_{n+1} = R_n + \delta R_n^{BL}$, $\Omega_n = \Omega_{n+1} + \delta\Omega_n$ and using Taylor-expansion, then the width of the BL is:

$$\frac{\delta R_n^{BL}}{R_n} \approx \frac{2}{5} \frac{\delta\Omega_n}{\Omega_n}. \quad (9)$$

δR_n^{BL} , $\delta\Omega_n$ here denote the width of the boundary layer between the SuSu-core and the ambient

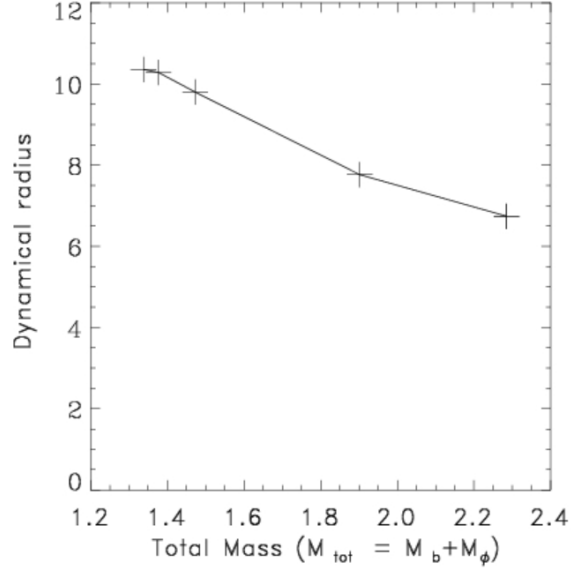


FIG. 8: The mass-radius relation of an evolving pulsar after selected glitch events. As the core becomes more massive, the Schwarzschild radius grows and converges asymptotically to the effective radius of the entire contracting object.

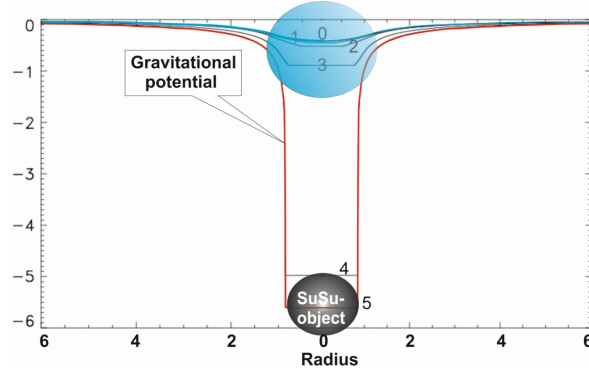


FIG. 9: The radial distribution of the gravitational potential shown for different epochs in the lifetime of the pulsar, which is equivalent to the radial projection of spacetime inside the SuSu-core governed by Minkowski spacetime, as well as in the surrounding region governed by the Schwarzschild metric. Obviously, as the object become more massive, it sinks deeper in spacetime, becomes gravitational redshifted to finally ends as an invisible dark energy object.

dissipative medium and the absolute difference between the rotational frequencies of the core before and after the glitch event, respectively.

Based thereon, the width of the BL during different evolutionary epochs of the pulsar may

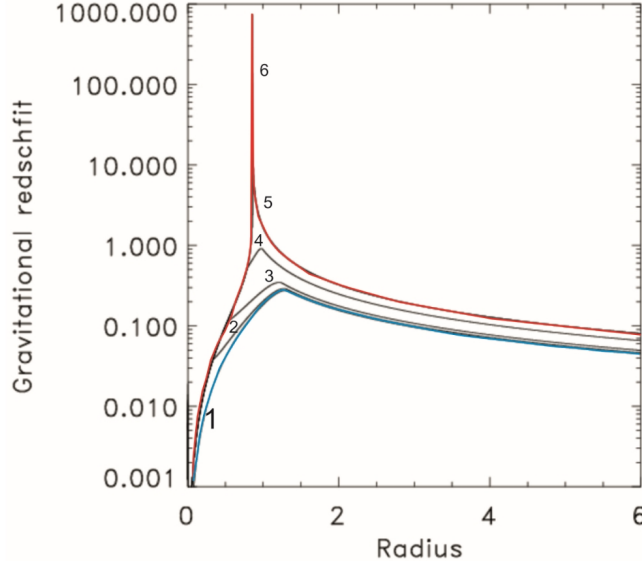


FIG. 10: The radial distribution of the gravitational redshift (Z) of the pulsar at different evolutionary epochs. Profile “1” corresponds to the low “ Z ” immediately after the pulsar was born, whereas Profile “6” depicts the divergent limit of “ Z ” at the surface of the object when it becomes completely invisible.

be estimated as follows:

$$\frac{\delta R_{BL}^n}{R_{SB}^n} \approx \begin{cases} 1.4 \times 10^{-10} & \tau_{age} = 0 \\ 2.2 \times 10^{-8} & \tau_{age} = 1000 \text{ yrs/Crab} \\ 1.6 \times 10^{-6} & \tau_{age} = 10000 \text{ yrs/Vela} \\ 3.8 \times 10^{-6} & \tau_{age} = 10 \text{ Myr}, \end{cases} \quad (10)$$

where τ_{age} stands for the age of the pulsar, provided the object is perfectly isolated and shielded from whatsoever external effects. In calculating the ratio at $\tau_{age} = 0$, the initial values $\alpha_c^{(n=0)} = 3.5 \times 10^{-10}$, $\Omega^{(n=0)} = 1400/s$ and $B^{(n=0)} = 10^{13}$ Gauss have been used (see [10] for further details). The values at $\tau_{age} = 1000, 10000$ yrs and $\tau_{age} = 10 \text{ Myr}$ are chosen to enable partial comparison with observations of the glitch events of Vela and Crab pulsars. On the other hand the numerical values have been selected from the sequence $\{\alpha_c^n\}$ displayed in Fig.(8) of [18].

For determining R_{SB}^n we use the current glitch-observation of the Vela and Crab and try to extrapolate them to other epochs. Following the analysis and Eqs. (13, 14, 15) in [18], the correlation of the inertia of the ambient dissipative media, I_{AM} , of the Crab and Vela pulsars reads:

$$I_{AM}^{Vela} \approx 10^{-2} I_{AM}^{Crab}, \quad (11)$$

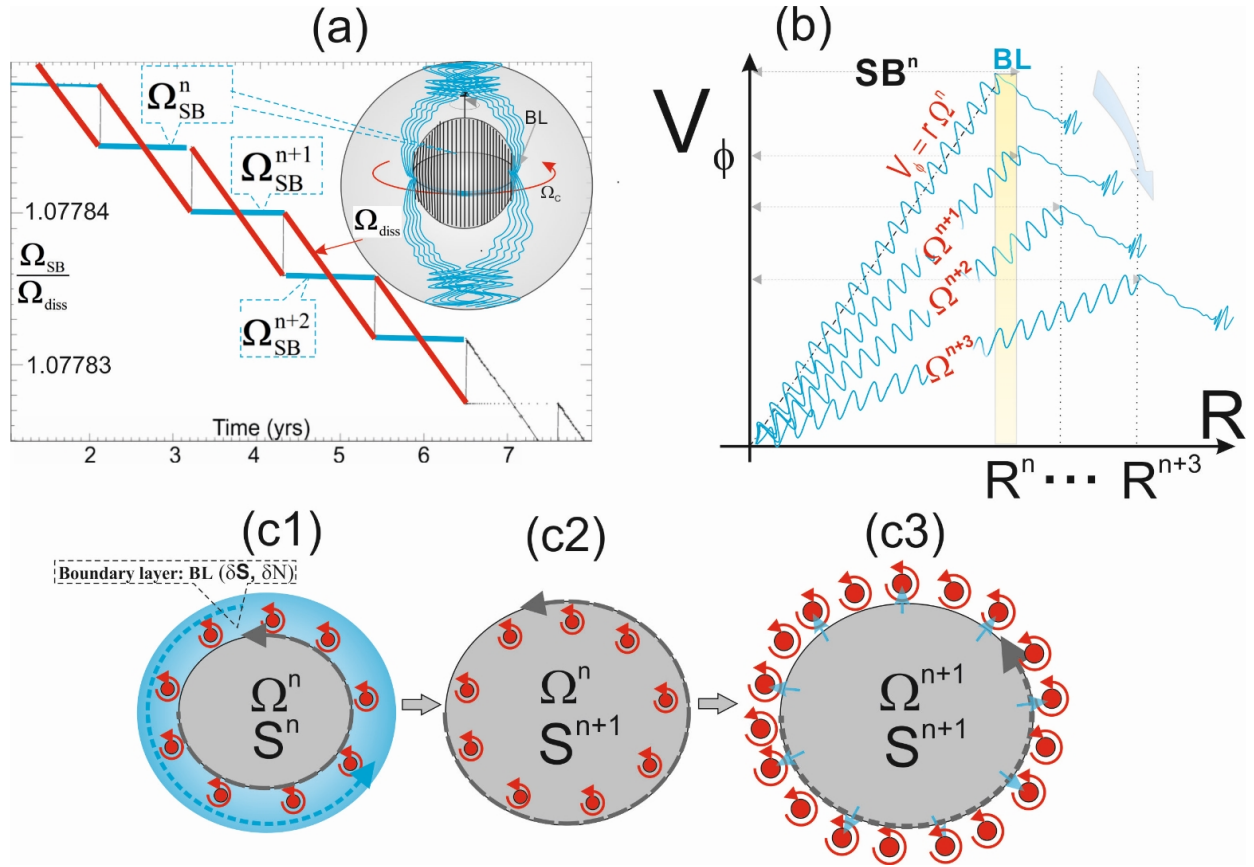


FIG. 11: The three-stage glitch scenario. In (a) the time-development of both rotational frequencies of the SuSu-core (blue-color) and of the ambient medium (red-color) are shown, using GR-numerical calculations. In (b) the rigid-body rotation and increasing size of the SuSu-core for four successive glitch-events are shown. The boundary layer here has the width δR , area δS and contains δN vortices. In the lower panel we show the three-stage scenario of the glitch phenomena in pulsars. In (c1) the SuSu-core and boundary at the verge of a glitch event are shown. Once the SNF has locked the neutrons inside the BL, to the core and enforced them to adopt the same thermo- and hydrodynamical properties of the matter inside the core, then the spacetime embedding the BL undergoes a topological change into a flat spacetime and merges with that of the core (c2). However, once the resulting difference $\Delta\Omega$ between Ω_{SB}^n of the core and the ambient medium Ω_{AM}^n has surpassed a critical value, then the core must undergo a transition into the next lower energy state by expelling a certain number of vortices (c3). In turn, the ambient medium absorbs the vortices and re-distribute them viscously, thereby giving rise to the prompt spin-up observed in glitching pulsars.

whereas the requirement that ejected rotational energy from the core of the Vela pulsar in the form of vortices should be observationally noticeable, implies that $R_{SB}^{now,Vela} \geq 10^{-2} R_{\star}^{Vela}$. This implies that $\delta R_{SB}^{now,Vela} \approx \frac{5}{2} R_{SB}^{now,Crab}$. Consequently, the cosmic values of R_{SB}^n can be summarized as follows:

$$\delta R_{SB}^n = \begin{cases} \mathcal{O}(10^{-7} \text{ cm}) & \tau_{age} = 0 \\ \mathcal{O}(10^{-4} \text{ cm}) & \tau_{age} = 1000 \text{ yrs}/Crab \\ \mathcal{O}(10^{-2} \text{ cm}) & \tau_{age} = 10000 \text{ yrs}/Vela \\ \mathcal{O}(1 \text{ cm}) & \tau_{age} = 10 \text{ Myr}, \end{cases} \quad (12)$$

An important question may be posed here:

What is the nature of force in the boundary layer that is capable of triggering glitches?

Here we argue that the strong nuclear force (SNF) is the deriving force that is capable of changing instantly both the physical properties of the quantum fluid as well as the topology of spacetime in the BL.

- Following [18], the core mimics a super-baryon (SB), in which the enclosed quarks are shielded by a gluon-cloud. The SB interacts then with overlaying supranuclear dense neutrons via vector mesons: the messengers of the SNF. In turn, the SNF locks the neutrons gradually to the core and enforces them to rotate rigidly with the core.
- The SNF generally operates effectively on nucleon length scales, i.e. when $\delta R_{BL}^n \approx R_{SB}^n = \mathcal{O}(1) \text{ fm}$. However, the inertia of a core of a neutron-size would be approximately 100 orders of magnitude smaller than that of the ambient medium. In this case, its rotational and thermal decoupling from the ambient medium would be almost impossible. On the other hand, in order for a SuSu-core to survive and affect the dynamics of the ambient medium, its inertia must have a minimum value. Here we recall that the initial frequency of a newly born pulsar is 1400 /s approximately [10]. In order for a SuSu-core to be able to eject one single vortex, its radius must be larger than 10^3 cm , hence its minimum mass: $\mathcal{M}_{SB}^{t=0} \geq 2.58 \times 10^{24} \text{ g}$. Indeed, the above tabulated values of δR_{BL}^n show that δR_{BL}^n correlates nicely with the size of the enclosed SuSu-core and it may even become of macroscopic size at the end of pulsars luminous lifetime.
- The essential question that rises is:

What keeps the core dynamically stable against the weight of the overly-

ing massive shells, or equivalently against compression by the surrounding strongly curved spacetime? As the gravitational potential inside the core is constant, then the medium has zero stratification due to gravity. In this case the only opposing force is the pressure gradient at the interface between SuSu-cores and the ambient compressible dissipative medium. The pressure gradient here could be seen as the repulsion force due to Pauli exclusion principle. In this case, one possible configuration would be to have the gluon-quarks uniformly distributed on the surface of the SuSu-core, forming thereby a surface tension that is capable of confining the quarks whilst opposing further compressions.

- As the neutron’s density in the BL approaches the critical value, ρ_{crit} , and as the chemical potential becoming closer to the upper-limit, μ_0 , the EOS should converge to $P \rightarrow a_0 \bar{n}^2$, where \bar{n} is the number density. This limiting EOS corresponds to purely incompressible fluids, implying therefore that the topology of the embedding spacetime must change into a flat spacetime. In this case, two instantaneous reactions in the BL are expected to occur (see Fig.11 a detailed description):
 - (a) The BL merges instantly with the SuSu-core to form a single quantum entity, thereby increasing its size and effective mass.
 - (b) The difference $\Delta\Omega = \Omega_n - \Omega_{n+1}$ between the rotational frequency of the combined BL-core system, i.e. the newly formed entity, and that of the ambient medium must have surpassed a critical quantum value. In this case, the system undergoes a transition into a lower energy state by promptly expelling a certain number of vortices into the ambient medium.
- Based on the here-presented scenario, the mechanisms underlying the glitch phenomena in pulsars and young neutron stars are due to dramatic changes of the physical conditions of the matter as well as of the topology of spacetime in the BL. Here the system operates on two different time scales: a relatively long times scale that correlates with size of the SuSu-core (e.g. approximately two year in the case of the Crab and Vela) and quantum events that occur instantly. The long-term changes can be listed as follows:

$$\overbrace{\text{Slow processes}}^{\tau_p \approx 2 \text{ yr}} : \left\{ \begin{array}{ll} EOS & \rightarrow P = \varepsilon \\ Compressible & \rightarrow Incompressible \\ Dissipative & \rightarrow Superfluid, \end{array} \right. \quad (13)$$

while the fast actions are:

$$\overbrace{\text{Fast actions}}^{\tau_p \leq 10^{-10} s} : \begin{cases} \text{Neutron fluid} \rightarrow \text{SuSu} \\ \text{Curved ST} \rightarrow \text{Flat ST} \\ E_{kin} \rightarrow \Downarrow E_{kin} \\ \Leftrightarrow \Downarrow N_{vortices}. \end{cases} \quad (14)$$

- As the ambient compressible and dissipative medium cools and spins down and subsequently converts into SuSu matter, the core becomes more massive and larger. By the end of luminous lifetime of the pulsar, the whole object should have entirely metamorphosed into a SuSu-object, thereby doubling its initial mass and yielding radius that roughly coincides the event horizon. For remote observers the object becomes practically invisible and therefore indistinguishable from stellar black holes.

This evolutionary scenario may explain nicely, why neither black holes nor neutron stars have ever been observed in the mass range $\{2.5 \mathcal{M}_\odot \leq \mathcal{M} \leq 5 \mathcal{M}_\odot\}$ as well as why the NS-merger in GW170817 [1] did not collapse into a stellar BH.

Acknowledgment The calculations have been carried out using the computer cluster of the IWR, University of Heidelberg. RS is supported by KAUST baseline research funds.

-
- [1] Abbott, B.P. et al. (2017), GW170817, Phys. Rev. Lett., Band 119, S. 161101
 - [2] Haensel, P., Potekhin, A.Y. & Yakovlev, D.G. (2007) "Neutron stars 1", Springer.
 - [3] Espinoza, C.M., Lyne, A.G., Stappers, B.W., Kramer, C. (2011) MNRAS, 414, 1679.
<https://doi.org/10.1111/j.1365-2966.2011.18503.x>
 - [4] Eya, I.O., Urama, J.O. (2014) Int. J. of Astrophysics and Space Science, 2, 16.
 - [5] LHCb Collaboration (2015) Physical Review Letters, 115, Article ID: 072001.
 - [6] Camenzind, M. (2007), Compact Objects in Astrophysics, Springer, Heidelberg
 - [7] Glendenning, N. (2007), Special and General Relativity. Springer, Berlin <https://doi.org/10.1007/978-0-387-47109-9>
 - [8] Hujeirat, A.A., Thielemann, F-K., (2009) MNRAS, 400, 903 <https://doi.org/10.1111/j.1365-2966.2009.15498.x>
 - [9] Yarmchuk, E.J., Gordon, M.J.V & Packard R.E. (1979) , Phys. Rev. Lett., 43,214

- [10] Haensel, P., Lasota, J.P., Zdunik, J.L. (1999) A&A, 344, 151
- [11] Bethke, S. (2007), Progress in Particle and Nuclear Physics, 351, 58
- [12] Cook, G.B., Shapiro, S.L., Teukolsky, S.A. (1994) ApJ Letters, 423, L117
- [13] Witten, E. (1984) Physical Review D, Volu. 30, Issue 2
- [14] Hujeirat, A.A. (2018). Journal of Modern Physics, 9, 51-69. <https://doi.org/10.4236/jmp.2018.91004>
- [15] Hujeirat, A.A. (2018), Journal of Modern Physics, 9, 70-83. <https://doi.org/10.4236/jmp.2018.91005>
- [16] Hujeirat, A.A. (2012) MNRAS, 423.2893
- [18] Hujeirat, A.A. (2018), Journal of Modern Physics, 9, 4, jmp.2018.94038
- [18] Hujeirat, A.A. (2018), Journal of Modern Physics, 9, 4, jmp.2018.94037
- [19] Miller, M.C. & Yunes, N., (2019) "The new frontier of gravitational waves"
- [20] Tanabashi, M. et al. Particle Data Group (2018), Phys. Rev. D 98, 030001
- [21] Ozel, F. & Freire, P. (2016), Annu. Rev. Astron. Astrophys., 54, 401
- [22] Walmsley PM, Golov AI, et al. (2007), Phys Rev Lett 99(26):265302
- [23] PHENIX Collaboration, (2019), Nature Physics, VOL 15, P 214220
- [24] Fischer, M., Hujeirat, A.A., (2019), in preparation